DOI: 10.1002/ejoc.201101736

Synthesis, Structure, and Photochemistry of 5,14-Diketopentacene

Tatsuya Aotake,[a] Shinya Ikeda,[b] Daiki Kuzuhara,[b] Shigeki Mori,[c] Tetsuo Okujima,[a] Hidemitsu Uno,[a] and Hiroko Yamada*[b,d]

Keywords: Pentacenes / Photochemistry / Soluble precursors / Ketones / Charge transfer

5,14-α-Diketopentacene, a structural isomer of 6,13-α-diketopentacene, was prepared from pentacene in three steps. In addition to the typical n–π* absorption of the diketone moiety at around 468 nm and the anthracene-like absorption at 333, 349, and 367 nm, a broad absorption was observed at around 386 nm, which could be assigned to an intramolecular charge-transfer absorption from anthracene to the diketone moiety. 5,14-α-Diketopentacene could be converted into pentacene quantitatively by photoirradiation at 405 and 468 nm in toluene with quantum yields of 2.3 and 2.4 %, respectively, and these values are higher than the quantum yield of 1.4 % obtained for 6,13-α-diketopentacene irradiated at 468 nm. The quantum yields in acetonitrile were lowered to 0.33 and 0.28 % with irradiation at 405 and 468 nm. The crystal structure of 5,14-α-diketopentacene showed a CH–π interaction and π–π stacking between neighbouring anthracene and benzene moieties. The lower solubility of 5,14-α-diketopentacene compared with the 6,13-isomer could be explained by this crystal structure.

Introduction

The acenes, which are polycyclic aromatic hydrocarbons composed of linearly combined benzene units, have fascinated organic chemists for more than a century.[1] In particular, pentacene (**PEN**) is currently used for applications in organic electronics, such as organic thin-film transistors (OTFT)[2–6] and organic thin-film photovoltaic cells.[7–10] For the manufacture of low-cost, easy-to-handle, printable devices, the solution processing of semiconducting materials is necessary. However, **PEN** is extremely insoluble in common organic solvents; thus, soluble precursors with thermally or photochemically removable leaving groups have merited increasing attention.[11–13] In this context, the photochemical conversion of an α-diketone precursor into anthracene (**Ant**) with the production of two CO molecules has been known for a long time (Scheme 1).[14] Irradiation of diketone (**DK**) compounds at the n–π* absorption leads to the release of two molecules of CO, and the corresponding acenes can be prepared quantitatively in solutions or in films. This reaction has recently been applied to the photochemical synthesis of **PEN** and larger acenes.[15,16] Such a photochemical method has enabled us to prepare a thin film by a solution process using the 6,13-α-diketone precursor of **PEN** (**6,13-DK**), followed by simultaneous treatment with visible light and mild heating. The thin film thus obtained exhibited top-contact OTFT with a mobility of 0.34 $cm^2 V^{-1} s^{-1}$ and an on–off ratio of 2.0×10^6. These values are comparable with those of devices prepared from thermally convertible precursors.[17] In 2011, we reported the α-diketone precursor of monoanthraporphyrins.[18] Photoirradiation of the Soret band of the porphyrin moiety induced decarbonylation of the connected α-diketone moiety, and monoanthraporphyrin was obtained. To use this mechanism in the **PEN** system, we have designed the 5,14-α-diketone precursor of **PEN** (**5,14-DK**), in which the **Ant**

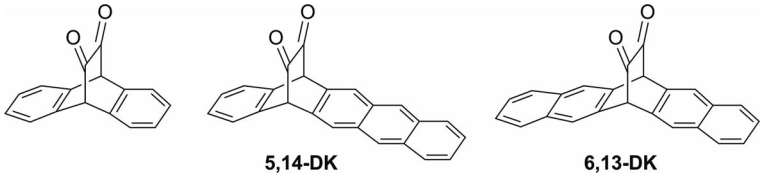

Scheme 1.

[a] Department of Chemistry and Biology, Graduate School of Science and Engineering, Ehime University, Matsuyama 790-8577, Japan
[b] Graduate School of Materials Science, Nara Institute of Science and Technology, Ikoma 630-0192, Japan
Fax: +81-743-72-6041
E-mail: hyamada@ms.naist.jp
[c] Department of Molecular Science, Integrated Center for Sciences, Ehime University, Matsuyama 790-8577, Japan
[d] CREST, JST, Chiyoda-ku 102-0075, Japan
Supporting information for this article is available on the WWW under http://dx.doi.org/10.1002/ejoc.201101736.

moiety has a moderate absorbance separate from the n–π* absorption, and therefore, the useful wavelength for photoconversion from the precursor to **PEN** will be broadened. Herein, we report the synthesis, crystal structures, and photoreactivity of **5,14-DK**.

Results and Discussion

Synthesis

The synthesis of **5,14-DK** is shown in Scheme 2. The Diels–Alder reaction of **PEN** with vinylene carbonate gave a mixture of 5,14 (**1**) and 6,13 adducts (**2**). After deprotection of the diol moieties, the mixture was separated by silica gel column chromatography to give the 5,14 (**5,14-PDO**) and 6,13 adducts (**6,13-PDO**) in 21 and 58%, respectively. Swern oxidation of **5,14-PDO** gave **5,14-DK** in 52% yield. The synthesis of **6,13-DK** has already been reported.[15a,15b]

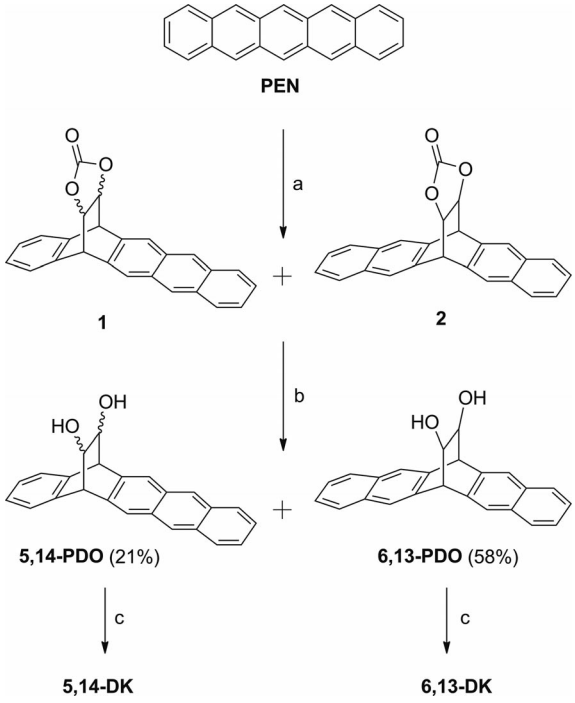

Scheme 2. Reagents and conditions: (i) vinylene carbonate, xylene, autoclave, 180 °C, 3 d; (ii) NaOH aq., dioxane, reflux, 2 h, 21% for **5,14-PDO** and 58% for **6,13-PDO** for 2 steps; (iii) trifluoroacetic anhydride, *N*,*N*-diisopropylethylamine, dry DMSO, dry CH_2Cl_2, –60 °C, 1.5 h, 52% for **5,14-DK** and 43% for **6,13-DK**.

Crystal Structure

An X-ray crystallographic measurement was performed on **5,14-DK** at 25 °C (Figure 1a).[19] The angles made by C(9)–C(10)–C(11) and C(16)–C(17)–C(18) were 107.6(2) and 106.7(1)°, respectively. The stacking pattern of the neighbouring molecules along the *c* axis in the crystal was also examined (Figure 1b). There was π–π overlap between two molecules. The distance between the **Ant** surfaces was 3.524 Å, which is shorter than that of the naphthalene–naphthalene distance of **6,13-DK** (3.596 Å). In general, the **Ant** has a stronger interaction between molecules than naphthalene. In **5,14-DK**, a similar interaction was observed between two molecules. The interaction was not only observed between **Ant** moieties, but also between the facing benzene rings. The distance between the surface of two benzene moieties was 3.849 Å. In addition, there was a CH–π interaction between hydrogen atoms and the neighbouring **Ant** moiety. The shortest contact between the hydrogen atoms and **Ant** surface was 2.767 Å. These interactions made the packing structure of **5,14-DK** rigid and lowered the solubility in common organic solvents. The solubility of **5,14-DK** in toluene was only 0.44 mg mL^{-1} at room temp., although it was 2.3 mg mL^{-1} for **6,13-DK**.

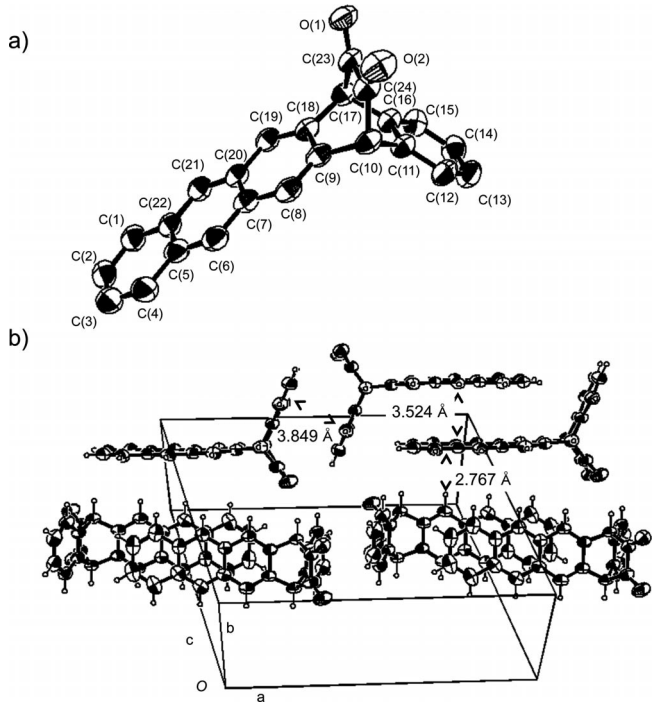

Figure 1. (a) ORTEP drawing of the X-ray structure of **5,14-DK** at 25 °C. Hydrogen atoms are omitted for clarity. Ellipsoids are drawn at the 30% probability displacement level. (b) Stacking pattern of neighbouring molecules.

Absorption Spectra

UV/Vis absorption spectra of **5,14-DK** and **6,13-DK**, along with the reference compounds **5,14-PDO**, **6,13-PDO** and **PEN**, in toluene are shown in Figure 2a. The absorption spectrum of **6,13-DK** showed an n–π* absorption of the **DK** moiety at 466 nm ($\varepsilon = 1.22 \times 10^3$ M^{-1} cm^{-1}) and a π–π* absorption at 329 (4.23×10^3 M^{-1} cm^{-1}) and 315 nm (4.05×10^3 M^{-1} cm^{-1}). The π–π* absorption peaks of **6,13-PDO** were 321 (1.41×10^3 M^{-1} cm^{-1}) and 306 nm (1.22×10^3 M^{-1} cm^{-1}). The π–π* absorption peaks of **6,13-DK** were broader and redshifted by 8 nm relative to those of **6,13-PDO**. For **5,14-DK**, a broad n–π* absorption of the **DK** moiety was observed at 464 nm (1.58×10^3 M^{-1} cm^{-1}), and a π–π* absorption of the **Ant** moiety was observed at

333 (5.49×10^3 M^{-1}cm^{-1}), 349 (5.40×10^3 M^{-1}cm^{-1}), and 367 nm (4.20×10^3 M^{-1}cm^{-1}). Furthermore, a broad absorption at 386 nm (2.98×10^3 M^{-1}cm^{-1}) was observed, although a similar peak was not observed for **6,13-DK**. The edge or broad band reached the n–π* absorption; therefore, the molar extinction coefficient of n–π* absorption of **5,14-DK** was larger than that of **6,13-DK**. Compared with the absorption of **5,14-PDO**, the π–π* absorption of the **Ant** moiety of **5,14-DK** was broadened and redshifted by 7–8 nm; this means the **Ant** moiety of **5,14-DK** strongly interacts with carbonyl moieties.

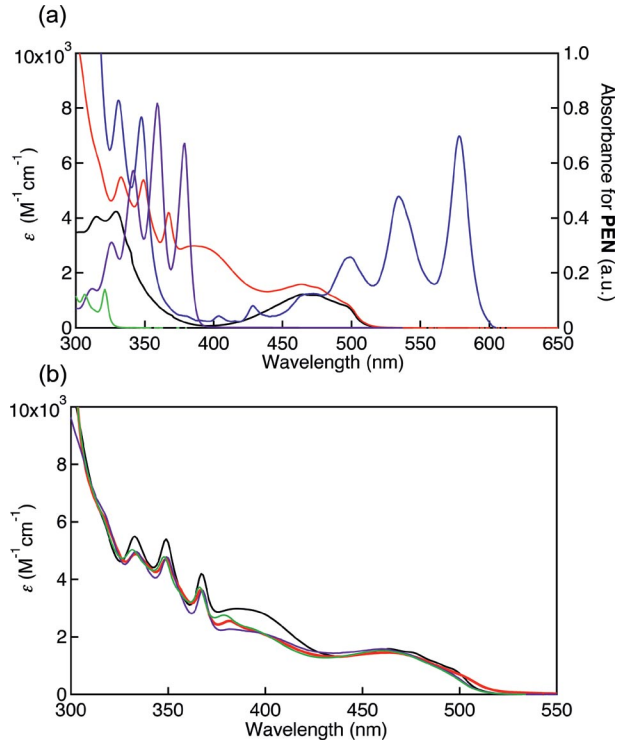

Figure 2. (a) UV/Vis absorption spectra of **5,14-DK** (red), **6,13-DK** (black), **PEN** (blue), **5,14-PDO** (purple), **6,13-PDO** (green) in toluene. (b) Solvent effect of **5,14-DK**. In toluene (black), in dichloromethane (red), in acetonitrile (purple), in DMF (green).

The absorption at 386 nm was characteristic of **5,14-DK** and was not observed for **5,14-PDO**. The absorption spectra of **5,14-DK** were measured from 1.79×10^{-1} to 7.39×10^{-3} mM in toluene, but a dependence on the concentration was not observed. These phenomena suggested that the absorption at 386 nm was an intramolecular charge-transfer (ICT) absorption from the **Ant** moiety to the **DK** moiety. To confirm this hypothesis, the absorption spectra of **5,14-DK** were measured in toluene, dichloromethane, acetonitrile and DMF (Figure 2b). In addition to the π–π* absorptions at 333, 349 and 367 nm, a vibrational peak at 375 nm was observed with shoulders at 400 nm in DMF. In acetonitrile and DMF, similar peaks were observed at 370 and 372 nm, respectively. The broad peak at 386 nm in toluene showed a clearer vibrational structure than that in other solvents; 382 nm (1.58×10^3 M^{-1}cm^{-1}) in dichloromethane, 382 nm (2.55×10^3 M^{-1}cm^{-1}) in DMF and 379 nm (2.75×10^3 M^{-1}cm^{-1}) in acetonitrile with shoulders around 400 nm. The n–π* and π–π* absorptions at 333, 349 and 367 nm showed a slight dependence on the solvent. The molecular extinction coefficients of the peaks at 333, 349 and 367 nm were smaller than those in toluene, but the peaks were observed at almost the same wavelength. On the contrary, with an increase in polarity of the solvents, the peak at 382 nm in dichloromethane was blue-shifted to 379 nm in acetonitrile. Therefore, these peaks were assigned not as the π–π* absorption but as the ICT absorption.

Such an intramolecular interaction was not observed for **6,13-DK**, probably due to the difference in HOMO levels of **Ant** and naphthalene. The energy gap between the HOMO of naphthalene and the LUMO of the **DK** moiety is larger than that between the HOMO of **Ant** and the LUMO of the **DK** moiety. Chow et al. reported 6,13- and 5,14-monocarbonyl **PEN**.[13] In their system, a CT-like absorption was not observed, because the n–π* transition is forbidden in the molecule and the molar extinction coefficient is very small. For **5,14-DK** and **6,13-DK**, the molar extinction coefficients of the n–π* absorption were over 1000, and the n–π* transition became possible to some extent.

Molecular orbital (MO) and time-dependent density functional theory (TD-DFT) calculations were performed for **5,14-DK** by using the Gaussian 09 program package at the B3LYP/6-31G(d)//CAM-B3LYP/6-31G(d) level of theory (Figure 3). The HOMO was localized on the **Ant** moiety, the LUMO on the carbonyl π* orbital and the HOMO-1 on the n orbital. TD-DFT calculations showed that the absorption at 456 nm corresponding to an n–π* transition that was mainly composed of the transition from HOMO-1 to LUMO (Figure S1 in the Supporting Information). Also, the absorption at 358 nm was calculated to be transitions from HOMO to LUMO or LUMO+1, which correspond to ICT from the **Ant** moiety to the **DK** moiety.

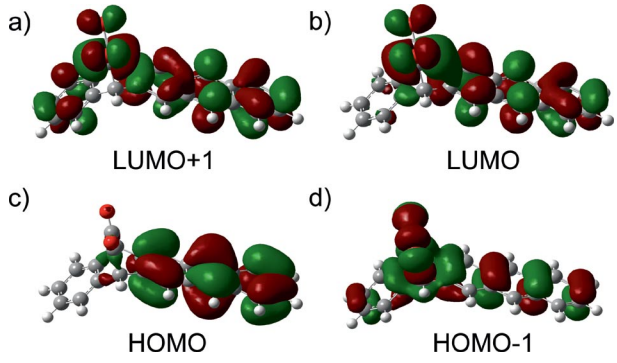

Figure 3. Molecular orbitals of (a) LUMO-1, (b) LUMO, (c) HOMO and (d) HOMO-1 of **5,14-DK** calculated at the B3LYP/6-31G(d)/s/CAM-B3LYP/6-31G(d) level.

Photoreaction

The photolysis reactions of α-diketone **5,14-DK** to **PEN** in argon are shown in Figure 4. Compound **5,14-DK** was irradiated at λ_{ex} = 405 and 468 nm. To monitor the photoreaction process, changes in the UV/Vis absorption spectra were measured every 30 s during photolysis. Firstly, a

1.1×10^{-1} mM solution of **5,14-DK** in toluene under argon was irradiated with light at 405 nm, as shown in Figure 4a. During irradiation, the peaks at 352–484 nm decreased gradually, and new peaks at 495, 530 and 578 nm increased. After the absorptions characteristic of **PEN** increased for 25 min, a purple solid appeared in the solution. As determined by observing the isosbestic points at 352 and 484 nm, the photoreaction proceeded quantitatively.

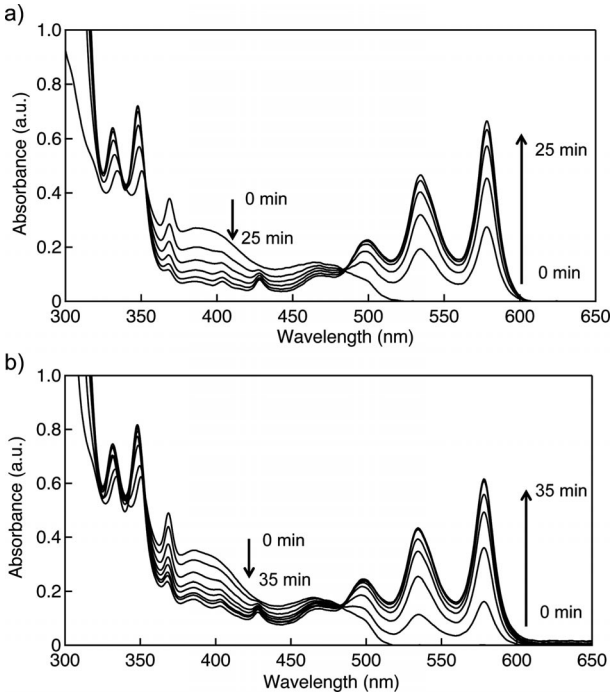

Figure 4. (a) Changes in the absorption spectra during photolysis (λ_{ex} = 405 nm) of **5,14-DK** in toluene. (b) Changes in the absorption spectra during photolysis (λ_{ex} = 468 nm) of **5,14-DK** in toluene.

Secondly, solutions of **5,14-DK** (1.3×10^{-1} mM) and **6,13-DK** (1.7×10^{-1} mM) in toluene under argon were irradiated with light at 468 nm, as shown in Figure 4b and Scheme 3. Similarly, the absorption spectra changed from the α-diketone to **PEN** with photoirradiation. The quantum yield (Φ_r) of the photoreaction of **5,14-DK** was measured by using potassium ferrioxalate actinomerty (Table 1). The Φ_r values of **5,14-DK** in toluene were 2.4 (λ_{ex} = 405 nm) and 2.3% (468 nm). The values are about two times that of **6,13-DK** (1.4%, 468 nm).

Table 1. Quantum yield of photoreactions of **5,14-DK** and **6,13-DK**.

	Φ_r [%] Toluene 405 nm[a]	468 nm[a]	Acetonitrile 405 nm [a,b]	468 nm[a,b]
5,14-DK	2.4 ± 1.0	2.3 ± 0.3	0.33 ± 0.13	0.28 ± 0.12
6,13-DK	–	1.4 ± 0.3	–	0.80 ± 0.10

[a] Excitation wavelength. [b] The ε value of **PEN** in acetonitrile was assumed to be the same as that in toluene.[20]

Next, photolysis reactions of **5,14-DK** and **6,13-DK** in acetonitrile were performed; the results are shown in Figure 5 and Figure S3 in the Supporting Information. In acetonitrile the photoreaction of **5,14-DK** was slower than that in toluene, and the Φ_r values were 0.28% for λ_{ex} = 468 nm and 0.33% for λ_{ex} = 405 nm, which are ten times lower than those in toluene. The Φ_r value of **6,13-DK** irradiated at 468 nm in acetonitrile was 0.80%; lower than that of 1.4% in toluene. Similar solvent-dependent behaviour of the reaction on the quantum yield was observed for the **DK**

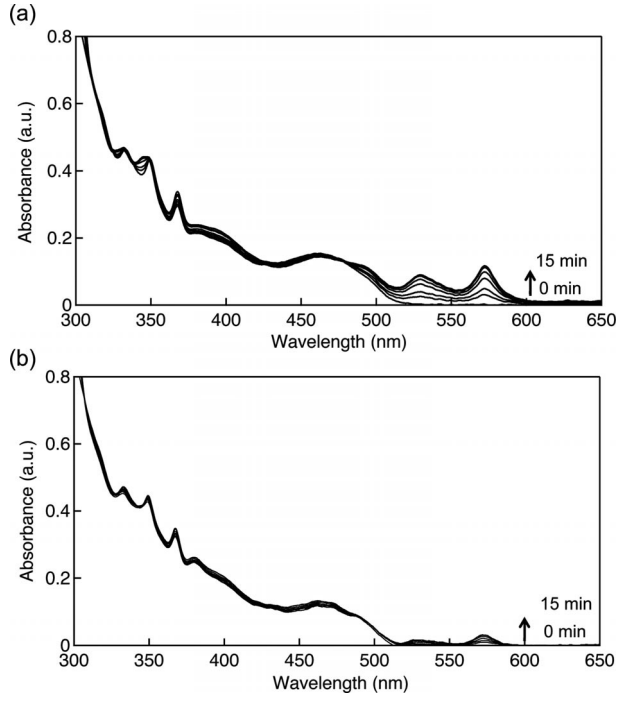

Figure 5. (a) Change in the absorption spectra during photolysis (λ_{ex} = 405 nm) of **5,14-DK** in acetonitrile. (b) Change in the absorption spectra during photolysis (λ_{ex} = 468 nm) of **5,14-DK** in acetonitrile.

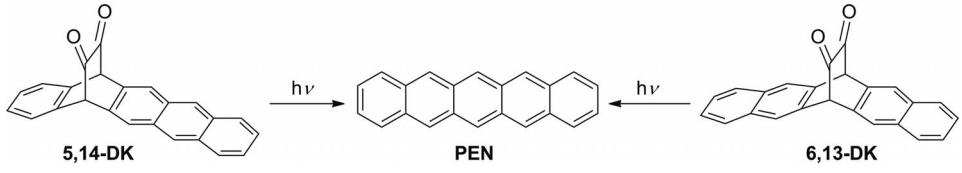

Scheme 3. Photochemical conversion of α-diketone **5,14-DK** and **6,13-DK**.

precursor of monoanthraporphyrin.[18] Compared with the photocleavage reaction in toluene, the occurrence of rapid photoinduced electron transfer from the singlet-excited-state porphyrin to the **DK** moiety in benzonitrile resulted in a significant decrease in the singlet-excited-state lifetime, leading to suppression of the photocleavage reaction.

The photoconversion reaction was also performed in a thin film. The UV spectra before and after photoirradiation are shown in Figure S4 in the Supporting Information along with photos of the thin film. The yellow film changed to purple during photoirradiation. However, the spectrum of **5,14-DK** was broad, and the band structures were not clear, probably due to π–π stacking of the compounds. The absorption spectrum of **PEN** was also broad, but the peaks characteristic for **PEN** were observed at around 560 and 610 nm.[15b]

Electrochemical Properties and Energy Diagrams

The electrochemical properties were measured in deaerated acetonitrile containing tetrabutylammonium hexafluorophosphate ($TBAPF_6$), as shown in Figures S5 and S6 in the Supporting Information. The one-electron reduction peak of **5,14-DK** was observed at –1.47 V (vs. Fc/Fc^+) for the reduction of the **DK** moiety. The oxidation peak was irreversible, and the peak maximum was at 0.94 V (vs. Fc/Fc^+), which corresponds to oxidation of the **Ant** moiety. The energy level of the charge-separated (CS) state ($\mathbf{Ant^{\cdot+}}$-$\mathbf{DK^{\cdot-}}$) was determined from the redox potential. The driving forces [$-\Delta G_{ET(CR)}$] for the intramolecular charge-recombination processes from the anion radical of the diketone moiety ($\mathbf{DK^{\cdot-}}$) to the cation radical of the anthracene moiety ($\mathbf{Ant^{\cdot+}}$) were calculated by using Equation (1):

$$-\Delta G_{ET(CR)} = e[E_{ox}(\mathbf{Ant^{\cdot+}/Ant}) - E_{red}(\mathbf{DK/DK^{\cdot-}})] \quad (1)$$

in which e stands for the elementary charge. On the other hand, the driving forces for the intramolecular charge-separation processes [$-\Delta G_{ET(CS)}$] from **Ant** to the diketone singlet excited state ($\mathbf{^1DK^*}$) were determined by using Equation (2):

$$-\Delta G_{ET(CS)} = \Delta E_{0-0} + \Delta G_{ET(CR)} \quad (2)$$

in which ΔE_{0-0} is the singlet excited state of the diketone moiety ($\mathbf{^1DK^*}$). The energy levels of $\mathbf{^1DK^*}$ and $\mathbf{^3DK^*}$ were calculated from the **Ant-DK** compounds already reported.[21] The $\mathbf{^1DK^*}$ and ICT [(**Ant-DK**)*] levels were higher than that of the CS state (–2.41 eV). Thus, electron transfer from the **Ant** moiety to the **DK** group may occur, affording the CS state, as shown in the α-diketone precursor of monoanthraporphyrins.[18] The CS state decays mainly to the ground state by radiationless deactivation. However, the CS state in toluene may be higher in energy than that in acetonitrile. Because of this, charge separation of **5,14-DK** is not favourable in toluene, and the quantum yield of the photoreaction is higher than that in acetonitrile (Figure 6).

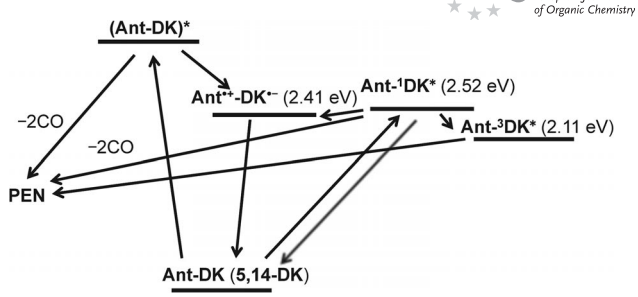

Figure 6. Energy diagram of **5,14-DK** in acetonitrile.

Conclusions

We successfully prepared **5,14-DK**, which is a photoconvertible precursor of **PEN** and a structural isomer of **6,13-DK**. Compound **5,14-DK** exhibited a broad ICT absorption at around 390 nm in addition to an n–π* absorption at 460 nm. Photochemical conversion to **PEN** quantitatively proceeded by photoirradiation at the ICT and n–π* absorptions in toluene, with quantum yields of 2.4 and 2.3%, respectively. However, the photoreaction in acetonitrile was slower, Φ_r = 0.33 (405) and 0.28% (468 nm), probably due to the occurrence of ICT from the **Ant** moiety to the **DK** group. X-ray single-crystal structure analysis of **5,14-DK** suggested that **5,14-DK** has a strong π–π interaction with neighbouring molecules, which lowers the solubility of **5,14-DK** in common organic solvents.

Experimental Section

General: Melting points were measured with a Yanaco M-500-D melting point apparatus. ^1H NMR and ^{13}C NMR spectra were recorded with JEOL JNM-AL 400 and AL 300 spectrometers at ambient temperature by using tetramethylsilane as an internal standard. FAB mass spectra were measured with a JEOL JMS-MS700 spectrometer. UV/Vis spectra were measured with a JASCO UV/Vis/NIR spectrophotometer V-570. Elemental analyses were performed with a Yanaco MT-5 elemental analyzer.

Materials: TLC and gravity column chromatography were performed on Art. 5554 (Merck KGaA) plates and silica gel 60N (Kanto Chemical), respectively. Acetonitrile was distilled from P_2O_5 in vacuo. All other solvents and chemicals were reagent-grade quality, obtained commercially, and used without further purification except as noted. For spectral measurements, spectral-grade toluene, dichloromethane, acetonitrile, and DMF were purchased from Nacalai Tesque.

Synthesis of 5,14-Dihydro-15,16-dihydroxy-5,14-ethanopentacene (5,14-PDO): A solution of **PEN** (1.00 g, 3.60 mmol) and vinylene carbonate (0.310 g, 3.64 mmol) in xylene (68 mL) was mixed at 180 °C in an autoclave for 3 d. After removal of the solvent in vacuo, the residue was washed with EtOAc to give a mixture of carbonate compounds (1.29 g). The mixture of carbonate compounds (1.29 g, 3.55 mmol) was added to a 4 M aqueous solution of NaOH and 1,4-dioxane (40 mL). The resulting mixture was heated at reflux for 1 h. The reaction mixture was cooled, poured into water, and then extracted with EtOAc. The combined organic layers were washed with water and dried with Na_2SO_4. After removal of the solvent in vacuo, the residue was purified by column chromatography on silica gel with EtOAc/$CHCl_3$ (1:4) to give **5,14-**

PDO (0.260 g, 0.770 mmol, 21%) as white crystals and 6,13-dihydro-15,16-dihydroxy-6,13-ethanopentacene (**6,13-PDO**; 0.710 g, 2.10 mmol, 58%). **5,14-PDO**: M.p. 275–277 °C. ^{1}H NMR (400 MHz, $CDCl_3$, TMS): δ = 2.18 (br., 2 H, OH), 4.23 (br., 2 H), 4.56 (br., 2 H), 7.25 (m, 2 H), 7.44–7.72 (m, 2 H), 7.89 (s, 2 H), 7.97–7.95 (m, 2 H), 8.33 (s, 2 H) ppm. ^{13}C NMR (100 MHz, $CDCl_3$, TMS): δ = 51.26, 68.81, 122.79, 125.11, 125.70, 126.54, 127.00, 127.88, 136.80 ppm. MS (FAB): *m*/*z* = 339 [M^+ + 1]. $C_{24}H_{18}O_2$ (338.41): calcd. C 85.18, H 5.36; found C 85.22, H 5.30.

Synthesis of 5,14-Dihydro-5,14-ethanopentacene-15,16-dione (5,14-DK): Trifluoroacetic anhydride (2.1 mL, 15.1 mmol) was added dropwise to a mixture of dry DMSO (1.0 mL, 14.0 mmol) and dry CH_2Cl_2 (10 mL) at –60 °C under argon. After stirring for 10 min, **5,14-PDO** (0.306 g, 0.905 mmol) dissolved in a mixture of dry DMSO (10 mL) and dry CH_2Cl_2 (7 mL) was added dropwise. After stirring for 90 min, *N*,*N*-diisopropylethylamine (4.50 mL, 25.8 mmol) was added dropwise to the reaction mixture. The solution was stirred at –60 °C for 60 min and warmed to room temp. before 3 M HCl (50 mL) was added to the mixture. The mixture was extracted with CH_2Cl_2, and the combined organic layers were washed with water and brine and dried with Na_2SO_4. After removal of the solvent in vacuo, the residue was purified by column chromatography on silica gel with CH_2Cl_2 and recrystallized from toluene to give **5,14-DK** as yellow crystals (0.157 g, 0.469 mmol, 52%). M.p. > 300 °C. ^{1}H NMR (400 MHz, $CDCl_3$, TMS): δ = 5.19 (s, 2 H), 7.39–7.41 (m, 2 H), 7.48–7.52 (m, 4 H), 7.99–8.01 (m, 2 H), 8.07 (s, 2 H), 8.42 (s, 2 H) ppm. ^{13}C NMR (75 MHz, $CDCl_3$, TMS): δ = 60.46, 125.45, 126.03, 126.36, 126.50, 128.13, 129.60, 130.95, 131.21, 132.16, 134.90, 184.84 ppm. MS (FAB): *m*/*z* = 336 [M^+ + 1]. $C_{24}H_{14}O_2$ (334.37): calcd. C 86.21, H 4.22; found C 86.50, H 4.59.

Theoretical Calculations: All DFT calculations were achieved with the Gaussian 09[22] program package. The geometry was fully optimized at the Becke's three-parameter hybrid functional combined with the Lee–Yang–Parr correlation functional abbreviated as the B3LYP level of density functional theory with 6-31G(d) basis set. Equilibrium geometries were verified by frequency calculations, where no imaginary frequency was found. Based on the B3LYP/6-31G(d)-optimized geometry, TD-DFT calculations were conducted at the CAM-B3LYP/6-31G(d) level of theory.[23]

Electrochemical Measurements: The cyclic voltammetry measurements of investigated compounds were performed with a BAS electrochemical analyser in deaerated acetonitrile containing nBu$_4$NPF$_6$ as a supporting electrolyte at 298 K (100 mV s^{-1}). The glassy carbon working electrode was polished with BAS polishing alumina suspension and rinsed with acetone before use. The counter electrode was a platinum wire. The measured potentials were recorded with respect to Ag/$AgNO_3$ and normalized to Fc/Fc^+.

Photochemical Reactions: The photocleavage reactions were carried out in a quartz UV cell, which was irradiated with monochromatic excitation light through a monochromator (Ritsu MC-10N) from a 500 W xenon lamp (Ushio XB-50102AA-A), and monitored by an OCEAN OPTICS HR-4000 high-resolution spectrometer system with light source DH-2000-BAL. A standard actionometer ($K_3[Fe(C_2O_4)_3]$)[24] was used for quantum yield determination of the photochemical reactions of **5,14-DK** and **6,13-DK** in acetonitrile and toluene. A square quartz cuvette (10 mm i.d.) that contained a deaerated solution (3.0 cm^3) of **5,14-DK** and **6,13-DK** was irradiated with monochromatized light (λ = 405 or 468 nm) through a monochromator (Ritsu MC-10N) by using a 500 W xenon lamp (Ushio XB-50102AA-A). Under the actinometry experimental conditions, both **5,14-DK** or **6,13-DK** absorbed essentially all incident light. The photochemical reaction was monitored by using a JASCO UV/Vis/NIR V-570 spectrophotometer. The quantum yields were determined from the increase in absorbance due to **PEN** (578 nm) at the beginning of the reaction.

Photochemical Reactions in Films: Compound **5,14-DK** (10 mg) was dissolved in hot $CHCl_3$ (1 mL), and the solution (100 μL) was spin-coated on glass at 1000 rpm for 20 s. The absorption spectrum of **5,14-DK** in the film was measured. Then the film was irradiated with a 460 W metal halide lamp through a blue filter in a glove box for 90 min, and the absorption spectrum of **PEN** was measured.

X-ray Analysis: Single crystals of **5,14-DK** suitable for X-ray diffraction analysis were obtained by slow diffusion of heptane into a solution of **5,14-DK** in CH_2Cl_2. The crystals were mounted in Litho Loops (purchased from Protein Wave). The diffraction data was collected at 25 °C with a Rigaku VariMaxRAPID/a imaging plate diffractometer with graphite-monochromated Cu-K_α radiation or with a Rigaku Mercury-8 diffractometer with graphite-monochromated Mo-K_α radiation equipped with a CCD detector. The diffraction data were processed with CrystalStructure of the Rigaku program, solved with the SIR-97 program,[25] and refined with the SHELX-97 program.[26]

Supporting Information (see footnote on the first page of this article):·TD-DFT calcuration, change in absorption spectra before and after photolysis in film, CV and DPV of **5,14-DK**; change in absorption spectra of **6,13-DK** during photolysis in solution.

Acknowledgments

We thank Prof. Atsushi Wakamiya, Institute of Chemical Research, Kyoto University for his valuable discussion on TD-DFT calculations. This work was partially supported by the Ministry of Education, Culture, Sports, Science and Technology (MEXT), Japan through a Grants-in-Aid (No. 22350083 to H. Y.) and the Green Photonics Project in NAIST sponsored by the Ministry of Education, Culture, Sports, Science and Technology, MEXT, Japan. Leigh McDowel is gratefully acknowledged for proofreading this manuscript.

[1] a) M. Bendikov, F. Wudl, D. F. Perepichka, *Chem. Rev.* **2004**, *104*, 4891–4945; b) J. E. Anthony, *Chem. Rev.* **2006**, *106*, 5028–5048.
[2] D. Knipp, R. A. Street, B. Krusor, R. Apte, J. Ho, *J. Non-Cryst. Solids* **2002**, *299–302*, 1042–1046.
[3] a) H. Klauk, M. Halik, U. Zschieschang, G. Schmid, W. Radlik, W. Weber, *J. Appl. Phys.* **2002**, *92*, 5259–5263; b) H. Klauk, M. Halik, U. Zschieschang, F. Eder, G. Schmid, C. Dehm, *Appl. Phys. Lett.* **2003**, *82*, 4175–4177.
[4] J. A. Nichols, D. J. Gundlach, T. N. Jackson, *Appl. Phys. Lett.* **2003**, *83*, 2366–2368.
[5] M. Kitamura, T. Imada, Y. Arakawa, *Appl. Phys. Lett.* **2003**, *83*, 3410–3412.
[6] D. Kumaki, M. Yahiro, Y. Inoue, S. Tokito, *Appl. Phys. Lett.* **2007**, *90*, 133511-3.
[7] S. Yoo, B. Domercq, B. Kippelen, *Appl. Phys. Lett.* **2004**, *85*, 5427–5429.
[8] J. Yang, T.-Q. Nguyen, *Org. Electron.* **2007**, *8*, 566–574.
[9] J. Sakai, T. Taima, T. Yamanari, Y. Yoshida, A. Fujii, M. Ozaki, *Jpn. J. Appl. Phys.* **2010**, *49*, 032301–7.
[10] K. Nomura, T. Oku, A. Suzuki, K. Kikuchi, G. Kinoshita, *J. Phys. Chem. Solids* **2010**, *71*, 210–213.
[11] a) A. R. Brown, A. Pomp, D. M. de Leeuw, D. B. M. Klaassen, E. E. Havinga, P. Herwig, K. Müllen, *J. Appl. Phys.* **1996**, *79*,

2136–2138; b) P. T. Herwig, K. Müllen, *Adv. Mater.* **1999**, *11*, 480–483.
[12] a) A. Afzali, C. D. Dimitrakopoulos, T. L. Breen, *J. Am. Chem. Soc.* **2002**, *124*, 8812–8813; b) A. Afzali, C. D. Dimitrakopoulos, T. O. Graham, *Adv. Mater.* **2003**, *15*, 2066–2069; c) K. P. Weidkamp, A. Afzali, R. M. Tromp, R. J. Hamers, *J. Am. Chem. Soc.* **2004**, *126*, 12740–12741; d) A. Afzali, C. R. Kagan, G. P. Traub, *Synth. Met.* **2005**, *155*, 490–494; e) D. Zander, N. Hoffmann, K. Lmimouni, S. Lenfant, C. Petit, D. Vuillaume, *Microelectron. Eng.* **2005**, *80*, 394–397; f) T. Akinaga, S. Yasutake, S. Sasaki, O. Sakata, H. Otsuka, A. Takahara, *Chem. Lett.* **2006**, *35*, 1162–1163.
[13] a) K.-Y. Chen, H.-H. Hsieh, C.-C. Wu, J.-J. Hwang, T. J. Chow, *Chem. Commun.* **2007**, *10*, 1065–1067; b) T.-H. Chuang, H.-H. Hsieh, C.-K. Chen, C.-C. Wu, C.-C. Lin, P.-T. Chou, T.-H. Chao, T. J. Chow, *Org. Lett.* **2008**, *10*, 2869–2872.
[14] J. Strating, B. Zwanenburg, A. Wagenaar, A. C. Udding, *Tetrahedron Lett.* **1969**, *10*, 125–128.
[15] a) H. Uno, Y. Yamashita, M. Kikuchi, H. Watanabe, H. Yamada, T. Okujima, T. Ogawa, N. Ono, *Tetrahedron Lett.* **2005**, *46*, 1981–1983; b) H. Yamada, Y. Yamashita, M. Kikuchi, H. Watanabe, T. Okujima, H. Uno, T. Ogawa, K. Ohara, N. Ono, *Chem. Eur. J.* **2005**, *11*, 6212–6220; c) Y. Zhao, R. Mondal, D. C. Neckers, *J. Org. Chem.* **2008**, *73*, 5506–5513; d) S. Katsuta, H. Yamada, T. Okujima, H. Uno, *Tetrahedron Lett.* **2010**, *51*, 1397–1400.
[16] a) R. Mondal, B. K. Shah, D. C. Neckers, *J. Am. Chem. Soc.* **2006**, *128*, 9612–9613; b) R. Mondal, R. M. Adhikari, B. K. Shah, D. C. Neckers, *Org. Lett.* **2007**, *9*, 2505–2508; c) R. Mondal, C. Tönshoff, D. Khon, D. C. Neckers, H. F. Bettinger, *J. Am. Chem. Soc.* **2009**, *131*, 14281–14289; d) C. Tönshoff, H. F. Bettinger, *Angew. Chem. Int. Ed.* **2010**, *49*, 4125–4128.
[17] A. Masumoto, Y. Yamashita, S. Go, T. Kikuchi, H. Yamada, T. Okujima, N. Ono, H. Uno, *Jpn. J. Appl. Phys.* **2009**, *48*, 051505–5.
[18] H. Yamada, D. Kuzuhara, K. Ohkubo, T. Takahashi, T. Okujima, H. Uno, N. Ono, S. Fukuzumi, *J. Mater. Chem.* **2010**, *20*, 3011–3024.
[19] CCDC-854777 (25 °C) contains the supplementary crystallographic data for this paper. These data can be obtained free of change from The Cambridge Crystallographic Data Centre via www.ccdc.cam.ac.uk/data_request/cif.
[20] H-H. Perkampus in *UV/Vis Atlas of Organic Compounds*, 2nd ed., VCH, Weinheim, **1992**, p. 652.
[21] R. Mondal, A. N. Okhrimenko, B. K. Shah, D. C. Neckers, *J. Phys. Chem. B* **2008**, *112*, 11–15.
[22] M. J. Frisch, G. W. Trucks, H. B. Schlegel, G. E. Scuseria, M. A. Robb, J. R. Cheeseman, G. Scalmani, V. Barone, B. Mennucci, G. A. Petersson, H. Nakatsuji, M. Caricato, X. Li, H. P. Hratchian, A. F. Izmaylov, J. Bloino, G. Zheng, J. L. Sonnenberg, M. Hada, M. Ehara, K. Toyota, R. Fukuda, J. Hasegawa, M. Ishida, T. Nakajima, Y. Honda, O. Kitao, H. Nakai, T. Vreven, J. A. Montgomery Jr, J. E. Peralta, F. Ogliaro, M. Bearpark, J. J. Heyd, E. Brothers, K. N. Kudin, V. N. Staroverov, R. Kobayashi, J. Normand, K. Raghavachari, A. Rendell, J. C. Burant, S. S. Iyengar, J. Tomasi, M. Cossi, N. Rega, J. M. Millam, M. Klene, J. E. Knox, J. B. Cross, V. Bakken, C. Adamo, J. Jaramillo, R. Gomperts, R. E. Stratmann, O. Yazyev, A. J. Austin, R. Cammi, C. Pomelli, J. W. Ochterski, R. L. Martin, K. Morokuma, V. G. Zakrzewski, G. A. Voth, P. Salvador, J. J. Dannenberg, S. Dapprich, A. D. Daniels, Ö. Farkas, J. B. Foresman, J. V. Ortiz, J. Cioslowski, D. J. Fox, *Gaussian 09*, Revision A.2, Gaussian, Inc., Wallingford, CT, **2009**.
[23] a) A. D. Becke, *Phys. Rev. A* **1988**, *38*, 3098–3100; b) A. D. Becke, *J. Chem. Phys.* **1993**, *98*, 5648–5652; c) C. Lee, W. Yang, R. G. Parr, *Phys. Rev. B* **1988**, *37*, 785–789.
[24] C. G. Hatchard, C. A. Parker, *Proc. R. Soc. London, Ser. B* **1956**, *235*, 518–536.
[25] A. Altomare, M. C. Burla, M. Camalli, G. Cascarano, C. Giacovazzo, A. Guagliardi, A. G. G. Moliterni, G. Polidori, R. Spagna, *J. Appl. Crystallogr.* **1999**, *32*, 115–118.
[26] G. M. Sheldrick, *Acta Crystallogr., Sect. A* **2008**, *64*, 112–122.

Received: December 2, 2011
Published Online: February 8, 2012

